Shear-induced reorganization of renal proximal tubule cell actin cytoskeleton and apical junctional complexes

Yi Duan*†, Nanami Gotoh*, Qingshang Yan*, Zhaopeng Du*, Alan M. Weinstein‡, Tong Wang*, and Sheldon Weinbaum†§

*Department of Cellular and Molecular Physiology, Yale University, 333 Cedar Street, New Haven, CT 06520; †Department of Biomedical Engineering, City College of New York, City University of New York, Convent Avenue at 140th Street, New York, NY 10031; and ‡Department of Physiology and Biophysics, Weill Medical College of Cornell University, 1300 York Street, New York, NY 10021

Contributed by Sheldon Weinbaum, June 2, 2008 (sent for review January 31, 2008)

In this study, we demonstrate that fluid shear stress (FSS)-induced actin cytoskeletal reorganization and junctional formation in renal epithelial cells are nearly completely opposite the corresponding changes in vascular endothelial cells (ECs) [Thi MM *et al.* (2004) *Proc Natl Acad Sci USA* 101:16483–16488]. Mouse proximal tubule cells (PTCs) were subjected to 5 h of FSS (1 dyn/cm^2) to investigate the dynamic responses of the cytoskeletal distribution of filamentous actin (F-actin), ZO-1, E-cadherin, vinculin, and paxillin to FSS. Immunofluorescence analysis revealed that FSS caused basal stress fiber disruption, more densely distributed peripheral actin bands (DPABs), and the formation of both tight junctions (TJs) and adherens junctions (AJs). A dramatic reinforcement of vinculin staining was found at the cell borders as well as the cell interior. These responses were abrogated by the actin-disrupting drug, cytochalasin D. To interpret these results, we propose a "junctional buttressing" model for PTCs in which FSS enables the DPABs, TJs, and AJs to become more tightly connected. In contrast, in the "bumper-car" model for ECs, all junctional connections were severely disrupted by FSS. This "junctional buttressing" model explains why a FSS of only 1/10 of that used in the EC study can cause a similarly dramatic, cytoskeletal response in these tall, cuboidal epithelial cells; and why junctional buttressing between adjacent cells may benefit renal epithelium in maximizing flow-activated, brush border-dependent, transcellular salt and water reabsorption.

brush border microvilli | cytosketal reorganization | fluid shear stress | proximal tubule epithelium | tight junction

Fluid shear stress (FSS) produced by renal tubular flow modulates tubular epithelial salt and water reabsorption as well as H^+ and K^+ secretion (1–5). In kidney proximal tubules, Schnermann *et al.*(1) demonstrated four decades ago that there was a nearly proportional change in Na^+ and HCO_3^- reabsorption with variations in glomerular filtration rates (GFRs), namely "Glomerulo-Tubular Balance." The physiological importance of this regulation is to prevent loss of solute after increases in GFR and to preserve the adequate distal delivery of sodium and fluid when GFR is reduced. This highly regulated intake of Na^+ and HCO_3^- depends on the polarized delivery of transporter proteins, such as the Na^+/H^+ antiporter (NHE3) and the H^+-ATPase, to the apical membrane (6, 7). Our *in vitro* microperfusion studies have shown that luminal flow modulates both NHE3 (8) and H^+-ATPase (3) activities, whereas disruption of the actin cytoskeleton by treatment with cytochalasin D (cD) abolished this flow-dependent behavior (8), indicating that an intact actin cytoskeleton is essential for proximal tubule cells (PTCs) to transmit flow-induced mechanical forces and subsequently modulate transport.

In PTCs, the actin cytoskeleton forms unique arrangements at both the apical and basal aspects of the cell that help to define the specialized structures and functions of these membrane domains. The apical membrane, distinguished by a tight junction (TJ), contains a brush border that includes microvilli (9) and a terminal web. The microvillar actin core is connected to the terminal web, a dense layer of short actin filaments that underlies the entire apical membrane of the PTCs. The terminal web is supported at its periphery by a bundle of actin filaments that form a girdle, a dense peripheral actin band (DPAB), around the cell at the level of the adherens junction (AJ), which is a major site of contact between neighboring cells. At the basal membrane, focal adhesions (FAs) anchor the cells to the extracellular matrix.

In contrast to vascular endothelial cells (ECs), the effect of FSS on cytoskeletal organization of cultured PTCs remains poorly understood. One recent study on mouse PTCs showed that these cells undergo a change in phenotype in response to FSS, and that there is a marked redistribution of filamentous actin (F-actin) (10). This study was limited to F-actin and was largely observational. Another finding on renal podocytes (11) demonstrated that FSS can cause lamellipodia formation and diminish both stress fibers and the presence of vinculin in FAs. FSS-induced PTC cytoskeletal reorganization and the coordinated remodeling of junctional complexes (TJs and AJs) have yet to be examined. In the present study, we exposed immortalized mouse PTCs to defined laminar FSS in a parallel flow chamber and performed immunostaining on the major proteins of the actin cytoskeleton, AJs, TJs, and FAs. The results show that PTCs respond to FSS with a cytoskeletal reorganization of both actin and junctional-related proteins which, surprisingly, is almost exactly opposite that observed in rat fat pad ECs exposed to FSS for the same duration (12). Furthermore, we demonstrate that a FSS of only 1.0 dyn/cm^2, 1/10 of the FSS used for ECs (12), can cause the formation of both TJs and AJs. These paradoxical observations are explained in terms of a conceptual "junctional buttressing" model that relates the cytoskeletal reorganization of actin to the redistribution of various junctional- and actin-associated proteins. Finally we suggest that the actin filament bundles within the microvilli act as mechanosensors for PTCs.

Results

FSS-Induced Actin Cytoskeleton Reorganization. Confluent PTCs were cultured for five days and then exposed to either 0 or 1 dyn/cm^2, which is equivalent to 30 nl/min in isolated single proximal tubule (8), of FSS for 5 h (12). After exposure, the cells were fixed, stained for F-actin, and examined by confocal

Author contributions: Y.D., A.M.W., T.W., and S.W. designed research; Y.D. and N.G. performed research; Q.Y. and Z.D. contributed new reagents/analytic tools; Y.D., A.M.W., T.W., and S.W. analyzed data; and Y.D., A.M.W., T.W., and S.W. wrote the paper.

The authors declare no conflict of interest.

§To whom correspondence should be addressed. E-mail: weinbaum@ccny.cuny.edu.

This article contains supporting information online at www.pnas.org/cgi/content/full/0804954105/DCSupplemental.

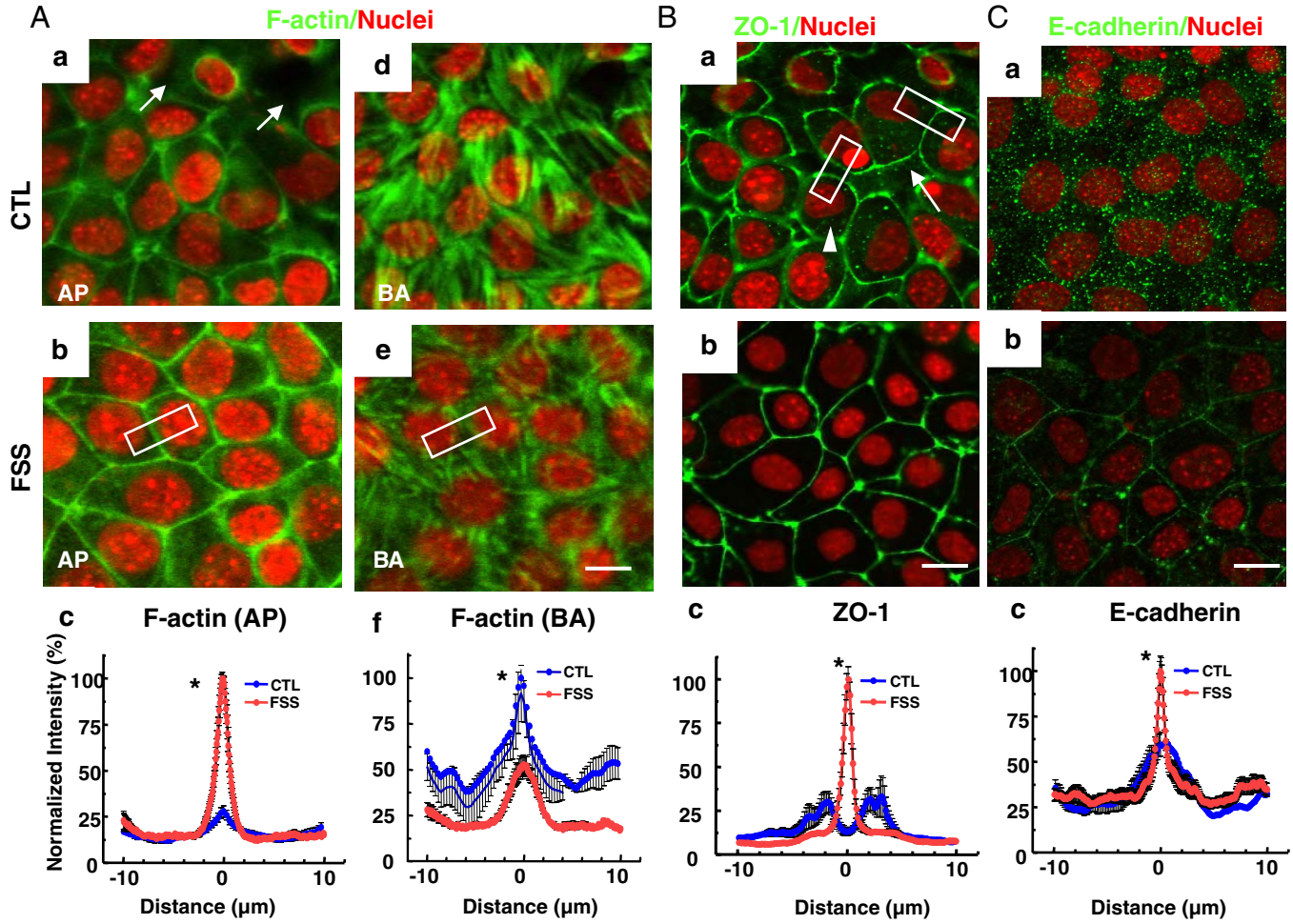

Fig. 1. Reorganization of confluent mouse PTC cytoskeleton and junctional complexes in response to FSS. PTCs were exposed to laminar FSS of 1 dyn/cm^2 for 5 h at 37°C. Effects of FSS on distribution of F-actin (*A*), ZO-1 (*B*), and E-cadherin (*C*) were analyzed by immunofluorescence confocal microscopy. Quantification of each protein distribution in cells under static control (blue) or FSS treatment (red) conditions was plotted by using ImageJ. Note the shift from bimodal to single-peak distribution signifying formation of TJs (*Bc*) and formation of peak intensity signifying formation of cadherin-related, AJ-associated DPABs (*Cc*). All data are presented as mean ±SEM, $n = 40$ (*, $P < 0.01$). Arrows, gaps between cells; arrowhead, intracellular localization; white rectangles, regions used to obtain average intensity profile; BA, cell base; AP, cell apex; CTL, control condition. (Scale bar, 10 μm.)

microscopy. Similar to the observations on PTCs in the FSS-induced phenotype study of Essig *et al.* (10), we witnessed a marked change in F-actin distribution. Fluorescein phalloidin staining showed the presence of two distinct and spatially separated actin microfilament populations, one located basally and the other apically. In the basal region of the no-flow treated cell, numerous long, thick cytosolic stress fibers were found that ran the entire length of the PTCs (Fig. 1*Ad*), which might be associated with cell-matrix interactions between the epithelium and substratum. Apically, microfilaments are organized into a relatively thin circumferential actin network at apical cell-cell contacts (Fig. 1*Aa*). In addition to the simple linear junctional outline in most areas, gaps between cells were frequently observed (Fig. 1*Aa*, arrows). Exposure of PTCs to FSS caused dramatically diminished, thick stress fibers at the basal surface (Fig. 1*Ae*); in addition, some short, randomly arranged actin bundles appeared throughout the cells. At this time, cells were found continuously apposed to each other at cell-cell junctions near the apical surface where we observed more prominent DPABs (Fig. 1*Ab*). The normalized fluorescence intensity at the apical junctional sites in the sheared cells was found to be significantly higher than in control cells for all four experiments (Fig. 1*Ac*; $p < 0.01$), whereas the intensity values in the basal region were significantly higher in the no-flow cells than in the sheared cells (Fig. 1*Af*; $p < 0.01$). A 5-fold increase in the magnitude of the FSS led to a more significant accumulation of actin filaments at peripheral cell borders near the apical surface (data not shown).

To test whether FSS affects total actin expression, we performed Western blot analysis and fluorescence line intensity analyses on the *XZ* images of actin staining [supporting information (SI) Fig. S1], see *SI Text*. The area under the intensity curve for control cells was 476, which was not significantly different from that of sheared cells (476. 3), see Fig. S1*B*. The Western blot results further confirmed that FSS only caused actin to shift from the basement membrane to the apical region without changing its total protein expression (Fig. S1*C*).

FSS-Induced TJ and AJ Formation. To investigate flow-stimulated TJ and AJ distribution, we examined the TJ-associated protein ZO-1 and the transmembrane AJ protein E-cadherin in PTCs. In the absence of FSS, ZO-1 did not form an apical cell-cell contact structure but appeared as isolated rings surrounding individual cells (Fig. 1*Ba*). This separation corresponds to the two outermost peaks in the intensity profile shown in Fig. 1*Bc* (blue). The cytosol also exhibited a certain amount of anti-ZO-1

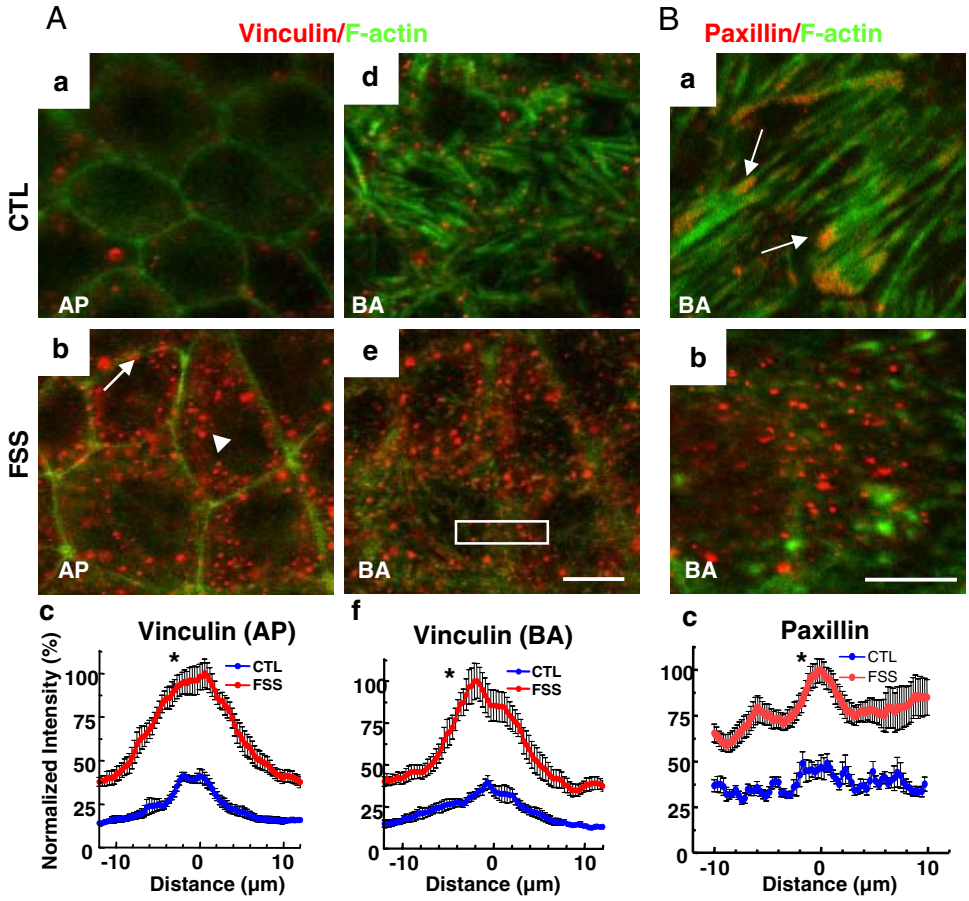

Fig. 2. Reorganization of the PTC cytoskeleton and FAs in response to FSS. (*A*) Distribution of F-actin (green) and vinculin (red) in control (*a* and *d*) and FSS-stimulated cells (*b* and *e*), whereas *c* and *f* show quantification of vinculin distribution in the absence (blue) or presence (red) of FSS. Note the large enhancement of vinculin distribution in both AP and BA regions. Arrow, vinculin localized at cell junction sites; arrowhead, nucleus periphery. (*B*) Localization of paxillin (red) in cells subjected to static control (*a*) or with FSS stimulation (*b*). Arrows, paxillin localized at the termination of stress fiber sites. Quantification of paxillin in the absence (blue) or presence (red) of FSS is shown in (*c*). Note the large enhancement of paxillin distribution, signifying the formation of basal focal attachments in response to FSS. All data are presented as mean ±SEM, $n = 40$ (*, $P < 0.01$). AP, cell apex; BA, cell base; CTL, control condition. (Scale bar, 10 μm.)

staining that appeared as dot-like structures (Fig. 1*Ba*, arrowhead). Exposure to 5 h of FSS induced a significant reassembly of intercellular junctions. After shear, a continuous distribution with a dramatically reinforced, junctional-staining pattern of ZO-1 was observed (Fig. 1*Bb*). Similarly, the majority of punctuate staining of intracellular E-cadherin at cell-cell interfaces in static culture became continuous and was localized at the position of cell-cell junctions after imposition of FSS (Fig. 1*C*). The intensity values at the junctional region for both proteins were significantly higher in the sheared cells than in the no-flow cells (Fig. 1 *B* and *Cc*; $p < 0.01$).

FSS-Induced FA Redistribution. Vinculin and paxillin, two adaptor proteins present in FAs, were examined to study the effect of FSS in the modulation of FAs. Double detection of vinculin with F-actin showed that under static conditions, vinculin was sparsely localized at the cell border near the basement membrane (Fig. 2*Ad*) and was either absent or weak at the apical surface (Fig. 2*Aa*). A dramatic reinforcement of vinculin staining (red) was found in the presence of FSS. In both regions, not only did vinculin localize along lateral cell membranes in a punctate pattern (Fig. 2 *A b* and *e*, arrow) but was also localized circumferentially around the nucleus (Fig. 2 *A b* and *e*, arrowhead). The fluorescence intensity profiles of both apical and basolateral side of the cells are shown in Fig. 2 *A c* and *f*, respectively. In control cells, the intensity profile was relatively flat, indicating that the vinculin distribution was uniform throughout the cell. In contrast, in cells stimulated with FSS, fluorescence intensity was markedly higher at both the periphery and interior of the cells. Paxillin, on the other hand, colocalized with F-actin at stress fibers ends under control conditions (Fig. 2*Ba*, arrows). After 5 h of FSS, a predominant up-regulation of paxillin was found (Fig. 2*Bb*). The intensity profile clearly delineated a FSS-induced increase in paxillin expression (Fig. 2*Bc*).

Possible PTC Mechanosensor. The following experiments focused on the diverse cytoskeletal responses of PTCs after exposure to FSS. How do PTCs detect the FSS? Many studies have suggested that the sensing apparatus is likely to be either cytoskeletal elements or a structure that is located at the apical membrane surface. Several candidates have been identified in various cell types. We mainly focused on the following three candidates: microvilli (8, 13), finger-like structures on the apical membrane of PTCs, which contain a core of actin filaments (9); primary cilia, which consist of a 9 + 0 arrangement of microtubules (14); and glycocalyx (12), a thin "cell coat" observed on the surface membranes of ECs. To confirm that each of these structures is present on the surfaces of PTCs, we used SEM and confocal microscopy. The SEM results showed that PTCs exhibited dome

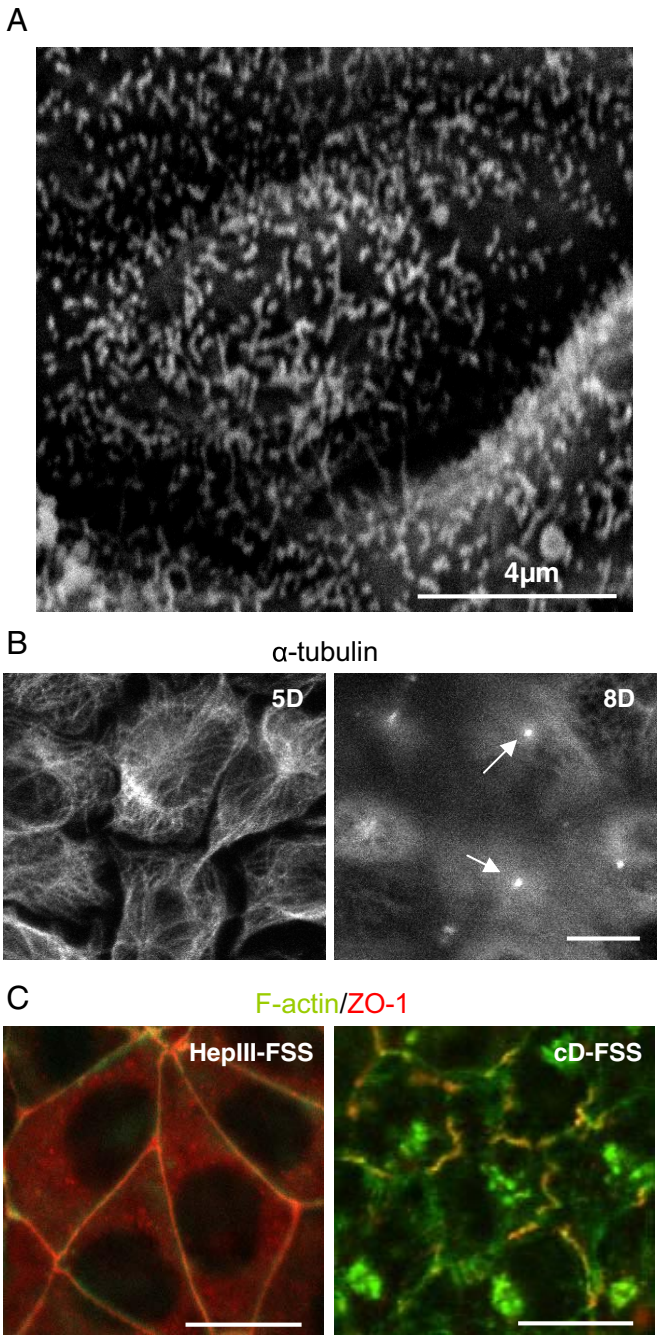

Fig. 3. Possible mechanosensor for mouse PTCs. (*A*) SEM picture of PTCs shows that the epithelium possesses numerous microvilli. (*B*) Antitubulin immunofluorescence staining of 5-d and 8-d cultured PTCs. Arrows, primary cilia. Note the complete absence of primary cilia at day 5 and formation at day 8. (*C*) Colocalization of F-actin (green) and ZO-1 (red) after exposed to 5 h of FSS in the presence of HepIII (*Left*) and cD (*Right*). Note that there was no difference in TJ formation (ZO-1) or appearance of AJs and DPABs after HepIII treatment, signifying that the glycocalyx plays an insignificant role in response to FSS. In contrast, both the TJs and the AJs were markedly disrupted by cD, indicating the primary role of F-actin in the cytoskeletal response to FSS. (Scale bar, 10 μm; otherwise as indicated.)

shapes with an apical domain bearing numerous microvilli (Fig. 3*A*). Then we stained for α-tubulin to investigate whether primary cilia are present in our cells. Interestingly, no cilia formed in PTCs cultured for five days (Fig. 3*B*) under conditions used in our FSS studies. However, after culturing the cells for eight days, primary cilia were observed protruding $\approx$2–3 μm above the apical membrane (Fig. 3*B*). This result ruled out the possibility that primary cilia could contribute to FSS-induced cytoskeletal reorganization of PTCs under our experimental conditions. Next, to test whether the glycocalyx or microvilli play a sensor role in regulating mechanotransduction in PTCs, we perfused the monolayer with the addition of heparinase III (HepIII) (to digest the glycocalyx) or cD (to disrupt the actin filaments) and analyzed the colocalization of both F-actin and ZO-1. Not surprisingly, we found that TJs still form after 5 h of FSS in the presence of HepIII (Fig. 3*C*). In comparison, cD treatment resulted in the disruption of actin filaments with the actin bundles reorganized into aggregates throughout the cytoplasm, as well as the discontinuous distribution of ZO-1, visualized as wavy ribbons at the cell borders (Fig. 3*C*). Clearly, TJs were not formed in the presence of cD.

Discussion

The experiments in this paper led to two important and unexpected observations. First, the cytoskeletal reorganization of F-actin and associated linker and junction proteins, in response to FSS in cultured confluent PTCs, is nearly diametrically opposite to that observed for ECs (12) that were also subjected to FSS for 5 h. In the latter paper, provided an intact glycocalyx was present, there was a DPAB, a few basal stress fibers, a dispersed distribution of vinculin, and a clearly defined continuous TJ in the control state as indicated by the localization of ZO-1. This organization was greatly altered after FSS with a breakdown of peripheral actin bands, a formation of stress fibers, a movement of vinculin to cell-cell adhesion sites at the basement membrane, and a disruption of TJs. These observations are opposite to those observed in the present study. Second, cultured PTCs, although confluent, do not form either AJs or TJs under control conditions. Quite remarkably, a FSS of only 1 dyn/cm^2 appears to be a critical precondition for the formation of both AJs and TJs. This FSS is only 1/10 of that applied in the EC reported study (12). The magnitude of the FSS would appear to be very significant because a FSS of 1 dyn/cm^2 is typical of PTCs *in vivo*, whereas a FSS of 10 dyn/cm^2 is more typical of ECs *in vivo*.

Another fundamental observation is that, in the case of ECs, the integrity of the glycocalyx layer is essential for the mechanotransduction of FSS. The experiments by Thi *et al.* (12) revealed that if the endothelial surface layer was compromised by either enzymatic treatment or the use of DMEM without plasma proteins, cytoskeletal reorganization was completely abolished, demonstrating that an intact glycocalyx plays a critical role in transmitting FSS to the underlying cytoskeleton. This result is explained in terms of a "bumper car" model, shown in Fig. 4 *A* and *B*, wherein the bending moment applied at the edge of the glycocalyx layer is instrumental in applying a rotational moment on the ECs, which leads to a disruption of the AJ and its peripheral actin band that functions much like a rubber bumper at the perimeter of the cell. The key observation in Fig. 4*B* is that the moment applied by the integrated, clockwise torque on the EC is resisted by an opposing moment applied at the AJ. When this moment exceeds the strength of the vascular, endothelial-cadherin bonds, there is a disruption of the AJ with a disassembly of the DPAB and a migration of vinculin to cell borders to form new basal attachments and stress fibers.

PTCs also contain a layer of acidic glycoproteins on the surface of brush border microvilli (15). However, this layer had little effect on the cytoskeletal reorganization in PTCs, in response to FSS, as shown in Fig. 3*C Left*. Our results indicate that the brush border microvilli on the apical surfaces of PTCs play the same role as the EC glycocalyx in that the fluid drag on these protuberances produces a rotational moment on the cell in response to FSS. Morphometric analysis revealed that the sur-

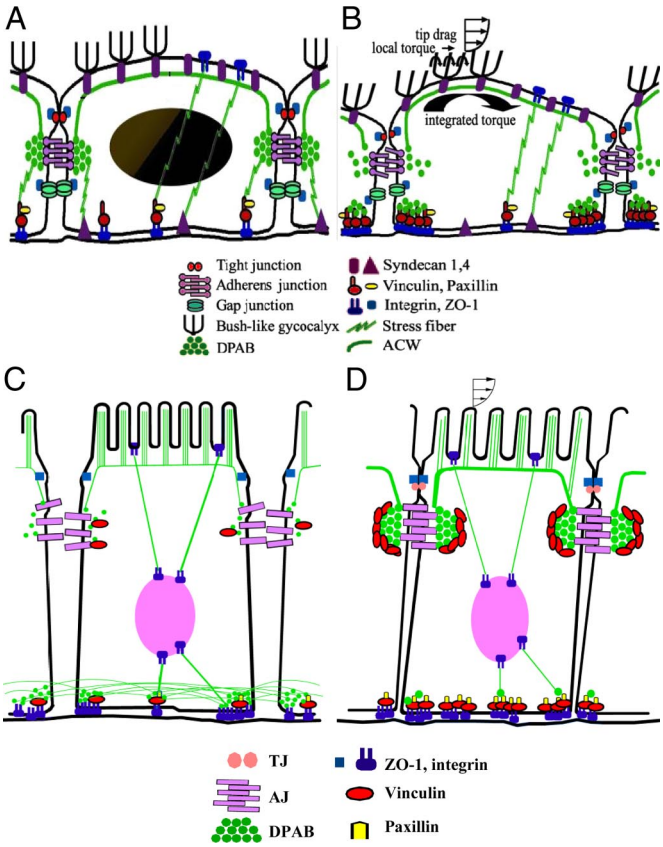

Fig. 4. A conceptual ''junctional buttressing'' model for the cytoskeleton reorganization and junctional formation of mouse PTCs in response to FSS in comparison with ''bumper-car'' model for ECs (12). (*A* and *B*) EC ''bumper-car'' model (previously published in ref. 12). (*A*) In control state , EC displays an intact DPAB that is localized to the AJ, functioning as a rubber fender of a bumper car that is constantly undergoing small collisions with its neighbors. (*B*) FSS causes a breakage of weak cadherin bonds, a disruption of AJs, and a disassembly of DPABs. (*C*) Regarding PTCs, there are neither AJs nor TJs under control conditions. These cells express numerous cytosolic stress fibers at their bases, which are in contact with one another at their periphery. This creates a tension in the membrane that pulls the membrane toward the base and forms a rounded canopy of cell membrane at the apical surface. (*D*) After exposure to FSS, stress fibers disappear from cell base and AJs, TJs, and DPABs form. More vinculin and paxillin accumulates at basolateral sites. Apically, more intense vinculin distribution was also found at the level of the AJ after 5 h of FSS.

face density of microvilli was $\approx 3.0/\mu m^2$ and their average height was ≈ 0.8 μm. This density is approximately one order of magnitude less than that found *in vivo*, where the microvilli form a highly organized, closely spaced, hexagonal array, and their height is $\approx 1/3$ that observed *in vivo* (9). The average spacing of microvilli in Fig. 3*A* is 0.55 μm and, thus, their spacing is nearly comparable to their height, allowing the flow to penetrate deep into the brush border. Therefore, the total force from the fluid flow that contributes to the rotational moment about the base of the cell includes two components, one from the drag on the microvilli and one from the FSS acting on the apical membrane. The combined moment is comparable to that *in vivo* where the rotational moment is, nearly exclusively, because of the drag acting on the tips of the microvilli at the edge of the brush border (outer 10%) (13), and the lever arms from the base of the cell are nearly the same for both force components.

Why do confluent ECs and PTCs respond in such a different manner to FSS? This can be explained with the aid of the conceptual ''junctional buttressing'' model shown in Figs. 4 *C* and *D*. In Fig. 4*C*, the PTCs are in a control state. As deduced from Fig. 1, under control conditions without flow, there are neither AJs nor TJs. The most important clue is the fact that the cells, although confluent and touching at their base, do not have TJs, as indicated by the distribution of ZO-1 in Fig. 1*B*. There is a strong expression of stress fibers at the base of the cell, as indicated by Fig. 1*A*, which causes a firm adhesion of the cell to its substrate. This creates a tension in the cell membrane, because of the compressive resistance of the internal cytoskeleton, which in turn produces a rounding of the apical surface and a pulling away of a cell from its neighbor at its basolateral surface. The cells have the appearance of tall cuboidal domes. Cell junctions cannot form until there is a disruption of the stress fibers at the basal surface and a release of this membrane tension. For the AJ to form, E-cadherin, in the vesicle-like structures observed in Fig. 1*C*, must form adhesive bonds between cells. Even a small FSS will cause these tall cuboidal cells to tilt and their basolateral surfaces to come into contact, as shown in Fig. 4*D*. This also causes a release of actin stress fibers at the basal surface and the formation of a DPAB as part of AJ assembly, as shown in Fig. 1*A*. In our experiments (data not shown), a higher FSS of 5 dyn/cm^2 was applied, and stronger peripheral actin bands were observed. Because adhesion of cells to matrix proteins is mediated by membrane receptors, particularly integrins, it is likely that the basal membrane of flow-stimulated PTCs was the site of accumulation or renewal of integrins. Vinculin and paxillin, which interact with newly recruited integrins at the FAs, appear to act as the new basal support for these tall epithelial cells.

The studies by Thi *et al.* (12) show that a much larger FSS is required to produce cytoskeletal reorganization in ECs. A threshold FSS of close to 10 dyn/cm^2 was needed to initiate remodeling, a value close to the measured physiological range. In contrast, a FSS of only 1.0 dyn/cm^2 is required for PTCs. This difference in FSS magnitude is largely because of cell geometry. Tall, cuboidal cells have large bending moments about their base, whereas the flat ECs appear to pivot about the plane of their AJs where their actin bumpers are in alignment, as seen in Fig. 4*A*, and the lever arm (distance from this plane) is much shorter. A second major difference is that in ECs, stress fibers extend from the basal to apical margins of the cell, providing for a direct structural link between forces applied at the apical surface to the FAs at the base. In PTCs, one expects that such direct links would be few in view of the tall, cuboidal geometry. Therefore, the need for stress fibers linking basal adhesions to the apical surface of the cell would be greatly reduced as observed in Fig. 1.

The current study identified the importance of FSS in the formation of TJs and AJs and the dramatic cytoskeletal reorganization in PTCs in response to FSS. This finding is important and could elucidate our understanding of FSS-induced proximal tubule transport mechanisms, as described (3, 8), for HCO_3^- and Na^+ reabsorption. The elucidation of the signal transduction pathway of FSS-induced cytoskeletal reorganization in PTCs and the identification of the elements involved in such a pathway may be helpful in further characterizing FSS-induced, cytoskeletal-related protein trafficking in PTCs. A possible role for the actin cytoskeleton has been suggested by Dubinsky *et al.* (16), who proposed that the cytoskeleton can mediate cross-talk between apical and basolateral transporters. The possibility is also quantitatively examined in the recent mathematical model by Weinstein *et al.* (17) for the overall tubular transport by using the microvilli torque hypothesis proposed in Guo *et al.* (13). Further studies are needed to investigate whether FSS-induced cytoskeletal reorganization favors membrane transporter protein trafficking in PTCs.

Materials and Methods

Cell Cultures. Mouse PTCs (provided by Dr. Lloyd Cantley, Yale University, New Haven, CT) were originally developed by John Schwartz, Boston University, Boston, MA (18) and were grown to confluence on glass coverslips coated with collagen. Two different types of culture conditions were used: (*i*) expansion at 33°C and (*ii*) differentiation at 37°C, as described (18, 19). Under expansion condition, cells were incubated at 33°C with renal tubular epithelial medium (DMEM/F12, 10% FBS, 100 U/ml penicillin, and 100 μg/ml streptomycin), supplemented with IFN-γ. For greater differentiation, cells were switched to 37°C three days before flow experiment in renal tubular epithelial medium only, no IFN-γ.

cD and HepIII Treatment. To identify the impact of physical modifications of the apical surface on the efficiency of flow-induced TJ formation, we treated the PTCs with two different enzymes: cD and HepIII. Fifteen units per milliliter HepIII (Sigma) were used to remove glycocalyx components (12), whereas 3 μM cD were added to inhibit the sensory system through brush border microvilli (8).

Flow System and Experiments. The flow system consisted of a parallel-plate, channel-flow chamber (Warner Instruments) and a programmable syringe pump (KD Scientific). This system produces laminar flow over the cell monolayer. A flow rate was chosen to yield a τ-value of 1 dyn/cm^2 by using the equation $\tau = 6\mu Q/bh^2$, where Q is flow rate, μ is medium viscosity, and b and h are channel width and height, respectively. Fluid temperature was maintained at 37°C.

To study the effect of steady laminar FSS on cytoskeleton reorganization, confluent PTC monolayers were exposed to laminar flow for 5 h with various perfusion solutions (serum-free culture medium, medium+Hep III, and medium+cD). Medium was incubated overnight with 5% CO_2. The 5-h flow-experiment duration was chosen based on conditions described by Thi *et al.* (12). Cells subjected to static control were kept in the incubator, and the cultured medium was changed every hour such that the total amount of exposed medium was the same as in the flow condition to eliminate the influence of cell metabolism accumulated in the medium. Each set of experiments was repeated four times.

Labeling of Cytoskeletal Structures. After exposure to laminar FSS, cells were stained with the following monoclonal antibodies: anti-ZO-1, E-cadherin, antivinculin, paxillin, and α-tubulin. F-actin was labeled by phalloidin, and the nucleus was labeled by To-PRO 3. The cells were fixed with PLP (8% paraformaldehyde, 0.1 M lysine, and 0.01 M sodium periodate in phosphate buffer, pH 7.4, 22°C), quenched for 15 min with 0.5 M ammonium chloride in 0.1% BSA-PBS, and then permeabilized with Triton X-100, blocked in serum buffer, and finally labeled with primary antibodies for 1 h. Alexa Fluor 488 or 594 goat anti-mouse IgG were used as secondary antibodies. The slide was covered with 15 μl Vectashield mounting medium (Vector Laboratories) and sealed with nail polish.

Fluorescence images were captured by using a confocal microscope (Zeiss, LSM 510). Z-stacks were performed by acquiring 10–12 images with a fixed 1-μm z interval at optimal confocal planes. Quantification of the fluorescence intensity profiles was analyzed by using ImageJ software (National Institutes of Health) for 30 cell pairs. Each cell pair was randomly selected at the *z* plane of interest (apical and basal region), within a region with a fixed range of 22 μm, with the apposition membrane approximately in the middle (12). In each of the seven paired images at the bottom of Figs. 1 and 2, the intensity data on the control and sheared cells were normalized by the maximum intensity at the midplane of the region, and all measurements were scaled relative to this maximum value, which was defined as 100% (20).

SEM. For SEM analyses, control PTCs were fixed in primary fixative (3% glutaraldehyde in 0.1 M sodium cacodylate and 0.1 M sucrose, pH 7.4), postfixed with osmium tetroxide, and dehydrated through an ethanol series. Fixed cultures were critical-point-dried with CO_2 as the transitional fluid, sputter-coated with gold-palladium (EMS, model 550), and then examined with an ISI SS40 SEM at 10 kV (Yale University).

ACKNOWLEDGMENTS. We thank Dr. Lloyd Cantley (Yale University) for providing the immortalized mouse PTC line. This work was supported by National Institutes of Health Grants R01DK62289-01 (to T.W. and S.W.) and R01DK29857 (to A.M.W.). This study was performed in partial fulfilment of Y.D.'s Ph.D. requirements for the City University of New York.

1. Schnermann J, Wahl M, Liebau G, Fischbach H (1968) Balance between tubular flow rate and net fluid reabsorption in the proximal convolution of the rat kidney. I. Dependency of reabsorptive net fluid flux upon proximal tubular surface area at spontaneous variations of filtration rate. *Pflugers Arch* 304:90–103.
2. Giebisch G, Windhager EE (1963) Characterization of renal tubular transport of sodium chloride and water as studied in single nephrons. *Am J Med* 34:1–6.
3. Du Z, *et al.* (2006) Axial flow modulates proximal tubule NHE3 and H-ATPase activities by changing microvillus bending moments. *Am J Physiol Renal Physiol* 290:F289–F296.
4. Malnic G, Berliner RW, Giebisch G (1989) Flow dependence of K+ secretion in cortical distal tubules of the rat. *Am J Physiol* 256:F932–F941.
5. Satlin LM, Sheng S, Woda CB, Kleyman TR (2001) Epithelial Na(+) channels are regulated by flow. *Am J Physiol Renal Physiol* 280:F1010–F1018.
6. Maddox DA, *et al.* (1992) Effect of acute changes in glomerular filtration rate on Na+/H+ exchange in rat renal cortex. *J Clin Invest* 89:1296–1303.
7. Preisig PA (1992) Luminal flow rate regulates proximal tubule H-HCO3 transporters. *Am J Physiol* 262:F47–F54.
8. Du Z, *et al.* (2004) Mechanosensory function of microvilli of the kidney proximal tubule. *Proc Natl Acad Sci USA* 101:13068–13073.
9. Maunsbach AB, Christensen EI (1992) *Handbook of Physiology: Renal Physiology*, ed Windhager, EE (Am. Physiol. Soc., Bethesda), pp 41–107.
10. Essig M, Terzi F, Burtin M, Friedlander G (2001) Mechanical strains induced by tubular flow affect the phenotype of proximal tubular cells. *Am J Physiol Renal Physiol* 281:F751–F762.
11. Friedrich C, Endlich N, Kriz W, Endlich K (2006) Podocytes are sensitive to fluid shear stress in vitro. *Am J Physiol Renal Physiol* 291:F856–F65.
12. Thi MM, Tarbell JM, Weinbaum S, Spray DC (2004) The role of the glycocalyx in reorganization of the actin cytoskeleton under fluid shear stress: A ''bumper-car'' model. *Proc Natl Acad Sci USA* 101:16483–16488.
13. Guo P, Weinstein AM, Weinbaum S (2000) A hydrodynamic mechanosensory hypothesis for brush border microvilli. *Am J Physiol Renal Physiol* 279:F698–F712.
14. Watanabe D, *et al.* (2003) The left-right determinant Inversin is a component of node monocilia and other 9+0 cilia. *Development* 130:1725–1734.
15. Roth J, Brown D, Orci L (1983) Regional distribution of N-acetyl-D-galactosamine residues in the glycocalyx of glomerular podocytes. *J Cell Biol* 96:1189–1196.
16. Dubinsky WP, Mayorga-Wark O, Schultz SG (1999) Volume regulatory responses of basolateral membrane vesicles from Necturus enterocytes: Role of the cytoskeleton. *Proc Natl Acad Sci USA* 96:9421–9426.
17. Weinstein AM, *et al.* (2007) Flow-dependent transport in a mathematical model of rat proximal tubule. *Am J Physiol Renal Physiol* 292:F1164–F1181.
18. Sinha D, *et al.* (2003) Chemical anoxia of tubular cells induces activation of c-Src and its translocation to the zonula adherens. *Am J Physiol Renal Physiol* 284:F488–F497.
19. Karihaloo A, *et al.* (2005) Vascular endothelial growth factor induces branching morphogenesis/tubulogenesis in renal epithelial cells in a neuropilin-dependent fashion. *Mol Cell Biol* 25:7441–7448.
20. Gerges NZ, Brown TC, Correia SS, Esteban JA (2005) Analysis of Rab protein function in neurotransmitter receptor trafficking at hippocampal synapses. *Methods Enzymol* 403:153–166.